Phase noise of an electro-optical phase modulator based electro-optical comb

BENEDIKT L. KRAUSE,[1,*] ANDREJ LAVRIČ,[2,3] JONAS TEBART,[3] ANDREAS STÖHR,[3] AND SASCHA PREU[1]

[1]Technical University of Darmstadt, Department of Electrical Engineering and Information Technology, Terahertz Devices and Terahertz Systems, Merckstr. 25, 64283 Darmstadt, Germany
[2]University of Ljubljana, Faculty of Electrical Engineering, Tržaška cesta 25, 1000 Ljubljana, Slovenia
[3]University Duisburg-Essen, Faculty of Engineering, Optoelectronics, Lotharstr. 55, 47057 Duisburg, Germany
[*]benedikt.krause@tu-darmstadt.de

Abstract: Photonic millimeter wave and terahertz frequency generation and detection benefit from a large tunability of several octaves as opposed to electronic frequency generation and multiplication. However, reaching multiple 100 GHz continuous tuning range while simultaneously featuring a linewidth in the Hz range and low phase noise is still very challenging. We present an electro-optical comb driving a photomixer with potential usability as an extension module based on side-band generation by an electro-optical phase modulator. This enables a Hz-level linewidth from microwaves to terahertz frequencies. We discuss the working principle of the mentioned electro-optical comb, characterize the phase noise of the optical subsystem up to frequencies of 40 GHz where electronic phase noise analyzers are available and draw conclusions on the phase noise at higher frequencies in the THz domain.

1. Introduction

Superheterodyne receivers found many use-cases since their development in the early 20$^{\text{th}}$ century [1] including radios, wireless communications, astronomy [2] and being part of measurement equipment i.e. spectrum analysers [3]. These receivers require a local oscillator (LO) providing a LO frequency and a mixer that mixes this frequency with the signal. Typically, mixers are based on diodes or transistors [4] and the LO has to emit at a similar frequency as the signal to be measured. Examples for LOs are voltage controlled oscillators [5], YIG-tuned oscillators [6], crystal oscillators [7] and atomic oscillators with stabilities in the order of and below 10^{-11} per month [8]. With additional synthesizers like phase locked-loops [9] or frequency multipliers based on diodes or transistors [10] these oscillators reach millimeter (mm) wave and terahertz (THz) frequencies. Between 2 THz and 5 THz quantum cascade lasers have been implemented [2]. In general, oscillators are subject to frequency fluctuations. These fluctuations can be translated from frequency to phase and are typically denominated as phase noise [11] which is one of the parameters used to describe the signal purity of the oscillator. Phase noise is a statistical process and therefore the spectral phase noise on both sides of the oscillation frequency is typically the same. Therefore, it is sufficient to measure the single side-band phase noise. A phase noise measurement determines the noise power at offset frequencies from the peak of the oscillation frequency. A low phase noise of electronic oscillators of $-105.72\,\mathrm{dBc/Hz}$ at 1 MHz was demonstrated at a center frequency of 58.48 GHz [12], $-107.5\,\mathrm{dBc/Hz}$ at 1 MHz at a center frequency close to 20 GHz [13] and $-110\,\mathrm{dBc/Hz}$ at 10 MHz at a center frequency of 176 GHz [14]. In contrast to classical electronic systems, photonic systems use an optical signal, e.g. around 1550 nm ($\sim$ 193 THz), that features at least two frequencies. A photomixer absorbs the laser signal in order to generate the LO frequency -being the difference frequency of these two colors- in form of a charge- or photocurrent modulation. The simplest implementation of this are two free-running continuous-wave (CW) lasers. As these are independent and just thermally stabilized they showcase a typical linewidth in the tens of kHz to the low MHz range [15] and thus large phase noise. The phase noise can be significantly reduced by referencing these two lasers either to themselves, to a high finesse cavity or to a frequency standard [16, 17]. Besides, optical frequency combs are a very low linewidth alternative. Phase noises as low as −108 dBc/Hz at 1 MHz at a center frequency of 560 GHz with a soliton comb [18] and −90 dBc/Hz to −95 dBc/Hz at 10 kHz at center frequencies of 330 GHz, 415 GHz and 500 GHz [19] have been achieved by locking CW lasers to pulsed frequency comb lines. While the first one is hardly tunable, the second one requires many expensive components.

In this paper we show that a relatively simple electro-optic (EO) comb also features excellent phase noise. EO combs generate multiple side bands on a single laser signal by EO phase modulation [20]. Originating from the same EO driver signal, the side bands show predominantly common noise such that mixing of any two side bands yields a signal with a spectral purity of the order of the radio frequency (RF) generator used to drive the EO comb. In a previous publication, we have shown that the linewidth is in the 1 Hz range [21], however, we had not analyzed its phase noise spectrum. The EO comb can be tuned by changing the RF or by selecting different side band combinations. We remark that all mentioned comb-based systems can reach THz frequencies [22, 23]. With the lack of a sufficient THz spectrum analyzer, we analyze the phase noise in this paper at 40 GHz where electronic measurement equipment is available. Section 2 discusses the difference frequency generation (DFG), section 3 estimates the phase noise contributions and section 4 showcases phase noise measurements under different settings with comparisons to the theory.

2. Electro-optical comb generation

For all of the considerations and measurements a fiber-coupled telecom-wavelength EO comb like the one presented in fig. 1 is used. This setup resembles a Mach-Zehnder interferometer [24].

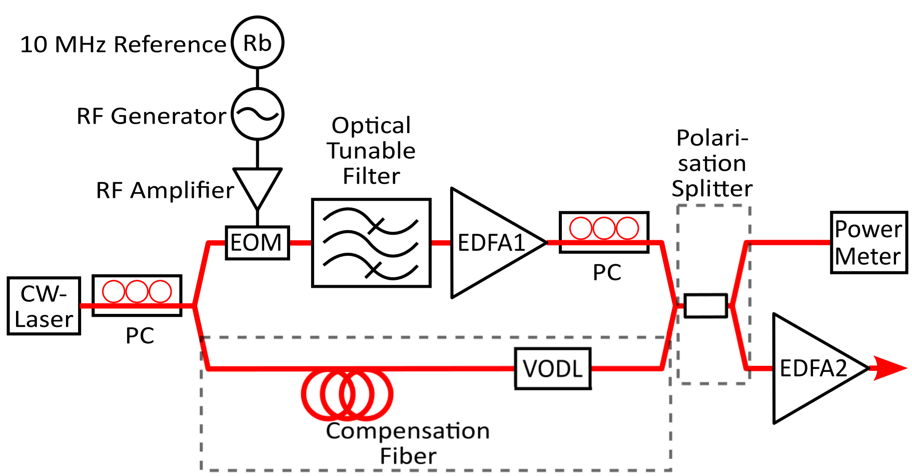

Fig. 1. Difference frequency generation setup with electro-optical phase modulator (EOM) -based EO comb. The Rubidium clock is optional. (CW - continuous-wave, PC - polarisation controller, EDFA - erbium doped fiber amplifier, VODL - variable optical delay line, Rb - Rubidium)

The continuous-wave (CW) laser generates a 1550 nm signal with an electrical field strength $E_\mathrm{L}(t)$ of $E_\mathrm{L}(t) = E_0 \mathrm{e}^{j\omega_\mathrm{L} t}$, where E_0 is the amplitude of the electric field and ω_L the laser frequency. A subsequent 3-dB coupler splits the signal in two paths. The upper path contains an electro-optical phase modulator (EOM), a tunable optical filter and an erbium-doped fiber amplifier (EDFA). The EOM is driven by an amplified radio frequency (RF) generator producing a sinusoidal signal with an angular frequency ω_{RF}. Thus, the EOM modulates the phase of the laser signal as

$$E_{\mathrm{EOM}}(t) = \frac{E_0}{\sqrt{2}}\eta_{\mathrm{EOM}}\mathrm{e}^{j(\omega_{\mathrm{L}}t+\gamma\sin(\omega_{\mathrm{RF}}t))} = \frac{E_0}{\sqrt{2}}\eta_{\mathrm{EOM}}\sum_{k=-\infty}^{\infty} J_k(\gamma)\mathrm{e}^{j(\omega_{\mathrm{L}}+jk\omega_{\mathrm{RF}})t} \tag{1}$$

where η_{EOM} is the optical insertion loss of the EOM and γ is the modulation depth given with

$$\gamma = \frac{\pi V_0}{V_\pi(\omega_{\mathrm{RF}})} \tag{2}$$

with the voltage applied to the EOM V_0 and its half-wave voltage V_π. The Jacobi-Anger expansion [25] at the right hand side of (1) shows that a sinusoidal modulated phase results in generation of side bands with a spacing of ω_{RF} whose strength decays with the k^{th} order Bessel function of the first kind, $J_k(\gamma)$. The modulation factor determines the strength of the different frequency components. A high modulation factor therefore generates more power in higher modes. η_{EOM} summarizes the optical losses within the EOM. The optical filter with an insertion loss at the pass band of η_{F} selects a single mode m. The EDFA with a gain of G_1 compensates for the losses by the components in the upper path, leading to a field of

$$E_{\mathrm{F}}(t) = \frac{E_0}{\sqrt{2}}G_1\eta_{\mathrm{EOM}}\eta_{\mathrm{F}}J_m(\gamma)\mathrm{e}^{j(\omega_{\mathrm{L}}+m\omega_{\mathrm{RF}})t} \tag{3}$$

In order to effectively cancel common noise in mixing the frequencies in the top and bottom path, both paths must be mutually coherent, i.e. their path length difference must be (much) smaller than the coherence length of the CW laser. Therefore, the bottom path only contains fiber including variable optical delay lines (VODL) with a total length compensating for the accumulated fiber lengths, yet with a small remaining phase difference $\Delta\varphi$ between the two. After combining both paths an additional EDFA with gain G_2 matches the power with the input requirements of the subsequent photomixer that now receives a heterodyned signal of

$$E_{\mathrm{comb}}(t) = \frac{E_0 G_2}{\sqrt{2}}\left[\eta_{\mathrm{EOM}}\eta_{\mathrm{F}}J_m(\gamma)G_1\mathrm{e}^{j(\omega_{\mathrm{L}}+m\omega_{\mathrm{RF}})t} + \mathrm{e}^{j(\omega_{\mathrm{L}}t+\Delta\varphi)}\right]. \tag{4}$$

The photomixer (either a photoconductor in the case of a photonic spectrum analyzer [15,21] or a p-i-n- diode as used in this paper) absorbs the laser signal resulting in a DC and AC charge carrier modulation, σ, that follows the optical beat note and acts as local oscillator,

$$\sigma \sim \left(\sigma_1 + \sigma_2 + 2\sqrt{\sigma_1\sigma_2}\cos\left(m\omega_{\mathrm{RF}}t + \Delta\varphi\right)\right) \tag{5}$$

$$\text{with } \sigma_1 = \eta_{\mathrm{PM}}\left(\frac{E_0}{\sqrt{2}}\eta_{\mathrm{EOM}}\eta_{\mathrm{Filter}}G_1G_2J_m(\gamma)\right)^2 \text{ and } \sigma_2 = \eta_{\mathrm{PM}}\left(\frac{E_0}{2}G_2\right)^2, \tag{6}$$

where c_0 is the speed of light, ϵ_0 the vacuum permittivity and η_{PM} is the photomixer's conversion efficiency. Maximising the THz component at $m\omega_{\mathrm{RF}}$ requires $\sigma_1 = \sigma_2$, hence $G_1 = (\eta_{\mathrm{EOM}}\eta_{\mathrm{Filter}})^{-1}$. η_{PM} is sensitive to the polarisation of the EO comb lines. As some components are non-polarization maintaining, we implement polarisation controllers (PC).

3. Phase noise considerations

In the following, we assume the phase noise contributions of the individual system components as independent although the statistical description of phase noise is non-trivial and there may be minor inter-dependencies [11, 26]. The top path experiences phase noise from the laser, ϕ_L, the RF generator with amplifier and the EOM, summarized as ϕ_{RF}, and both EDFAs, $\phi_{EDFA,j}$ while the bottom path is only affected by the laser and the second EDFA. We remark that the filter may indeed reduce noise as it suppresses out-of-band noise. The passband width of optical filters, however, is typically at least a few GHz wide and thus about 3 orders of magnitude wider than the frequency range typically investigated around the main peak in phase noise measurements. We therefore disregard effects of the optical filter on noise. The laser phase noise in both paths are correlated but may not completely cancel out for imperfect path length compensation. In the following, we express the relative time delay caused by the path length difference between the two paths as τ. The instantaneous phases for both frequency components become

$$\phi_1(t) = \phi_L(t) + |m|\phi_{RF}(t) + \phi_{EDFA1}(t) + \phi_{EDFA2}(t) \tag{7}$$

$$\phi_2(t) = \phi_L(t-\tau) + \phi_{EDFA2}(t) \tag{8}$$

As the photoconductor generates the difference frequency signal, only phase differences survive, leading to a LO phase of

$$\phi_{DF}(t) = \phi_L(t) - \phi_L(t-\tau) + |m|\phi_{RF}(t) + \phi_{EDFA1}(t). \tag{9}$$

We remark that the frequencies in both paths are slightly different which may, in principle, lead to different phase noise in common components, e.g. in EDFA2, as its noise floor is wavelength-dependent. For THz generation, the two tones are considerably close and we therefore omit non-common phase noise originating from EDFA2. Due to wavelength-dependent gain, there may be excess amplitude noise. In addition to the aforementioned noise sources the photomixer (photoconductor or p-i-n diode) attached to the EO comb adds thermal noise caused by its resistance which is predominantly white. The photocurrent noise floor of photoconductors measured in Terahertz homodyne systems is in the range of a few pA$\sqrt{\text{Hz}}$ at an illuminated resistance in the range of 5 kω_{RF} to 50 kω_{RF}. The resulting noise spectral density should therefore be (much) smaller than the noise sources addressed in this manuscript. The phase noise, resulting from fluctuations of the phase in 9, is typically measured at the single side-band (SSB) in the frequency domain, $L(f) \sim (\phi_{DF}(f))^2$. Its power spectral density is

$$L_{DF}(f) = |m|^2 L_{RF}(f) + L_{EDFA1}(f) + L_L(f,\tau) + L_{PCA}(f) = |m|^2 L_{RF}(f) + L_{opt}(f), \tag{10}$$

where $L_{PCA}(f)$ accounts for the photoconductor noise. From Eq. 10 we can draw two conclusions: (i) For perfect path length compensation, i.e. $\tau = 0$, the phase of the laser, including its noise contribution, perfectly cancels. The predominant noise source in this case is the RF system whose noise is typically orders of magnitude smaller than that of the free running CW laser. If τ becomes much larger than the coherence time of the CW laser then the phases in both paths become uncorrelated and will just add up, resulting in twice the laser's phase noise. Therefore, the path lengths have to be matched. For free running lasers, the coherence length is of the order of several meters, so a minor (almost inevitable) mismatch of pathlengths in the cm range can be tolerated. (ii) As the RF ω_{RF} is tunable and the system permits to pick any side mode order m, any LO frequency $f_{LO} = m\omega_{RF}/(2\pi)$ can be generated in several ways (e.g. $m' = 2m$ and $\omega'_{RF} = \omega_{RF}/2$). The phase noise of the RF generator typically scales quadratically with the operation frequency. Yet, as Eq. 10 consists of an RF noise contribution that scales with the square of the side band order but noise originating from optical components and the photoconductor that remains independent of the side mode order, we expect a sub-quadratic increase of noise with side mode order.

4. Phase noise analysis of the photonic LO

The EO comb system consists of the following components: a distributed feedback laser diode Profile WDM source at 1542.88 nm emitting an optical power of 13 dBm, an EOSpace PM-OS5-

20-PFA-PFA EOM, a Rohde & Schwarz SMP02 RF generator, referenced to a 10 MHz Rubidium (Rb) clock (Rohde & Schwarz XSRM with XSRM-Z), a HP8349B RF amplifier, a Yenista Optics XTA-50 tunable filter with the filter bandwidth set to 50 pm, an Amoco Laser Company L5-Amp as EDFA1, and a Pritel, Inc. optical fiber amplifier PMFA-35-S-10 as EDFA2. The bottom path contains two VODLs (OZ Optics ODL-650-11-1550-8/125-P-60-3A3A-1-1-MC/RS232-330). The output power of the RF generator is set to 10 dBm resulting in a total output power between 20 dBm and 27 dBm after the RF amplifier. Except the optical filter and EDFA1 all of components and fibers are polarisation maintaining. The polarisation is monitored at the second output of the polarizing beam splitter with a Sainsonic OP-600 optical power meter. By adjusting both PCs the undesired polarisation was suppressed to values below −10 dBm for all measurements, i.e. resulting in a polarisation suppression of at least 95 %. In order to analyze the phase noise of the photonic LO, we connect a fast photodiode (u^{2}t XPDV2120R) to the EO comb followed by a low noise amplifier (MiniCircuits ZVA-403 GX+). Its output is fed to a RF phase noise analyser (Rohde & Schwarz FWSP). To check the optical output power of the EO comb an inline optical power meter (Neo Photonics) is placed in between the output of the EO comb and the photodiode.

Table 1 summarizes the settings of the EO comb devices. We chose to use the sidebands above the centre wavelength of the laser with the filter. Please note that the calibration of the centre wavelength of the optical filter has a systematic offset error of up to 200 pm. The power of the EDFA1 is set to match the power of the selected mode with the power at the laser wavelength in the bottom path. Its setting ranges from 0 to 1 and scale with its current. The output power of EDFA2 is 10 dBm.

Table 1. Measurement settings for the showcased difference frequencies.

Difference frequency	RF frequency	Optical mode	Optical filter centre wavelength	EDFA1 power setting
10 GHz	10 GHz	1	1542.917 nm	0.163
20 GHz	10 GHz	2	1543.004 nm	0.142
30 GHz	10 GHz	3	1543.085 nm	0.168
40 GHz	10 GHz	4	1543.167 nm	0.214
40 GHz	$13.\bar{3}$ GHz	3	1543.155 nm	0.200
20 GHz	20 GHz	1	1543.003 nm	0.147
40 GHz	20 GHz	2	1543.155 nm	0.203

4.1. Fiber compensation length

In a first step, we optimized the compensation fiber length in the bottom path. From preliminary work we estimate the combined fiber length of the EOM, optical fiber, EDFA1 and PC to about (33.6 ± 0.1) m. Fig. 2 shows the resulting phase noise at fiber compensation lengths from 31.11 m to 35.45 m. We state an absolute error of at least 5 cm as the length of the VODLs is only estimated from its size and time delay setting and the lengths of the used fibers may vary slightly from their stated length. The increase of phase noise due to remaining laser noise is evident. The lengths between 33.51 m and 33.65 m show the lowest phase noise. Between these lengths the phase noise difference is smaller than the run-to-run deviation. In the following, we used the mean between these two values, i.e. 33.57 m. The phase noise difference of the longer compensation fiber lengths increases confirming imperfect noise cancelling of the correlated laser phase noise at large values of τ.

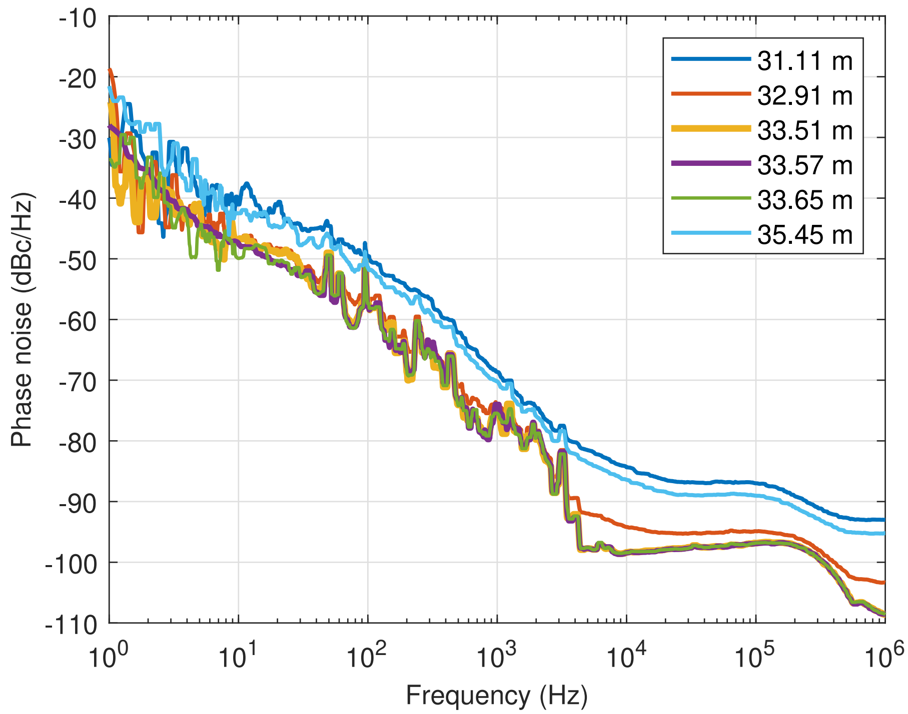

Fig. 2. Measured phase noise for different compensation fiber lengths at a difference frequency of 40 GHz using the second optical mode.

4.2. Referencing and amplitude noise

For all of the following measurements the phase noise is acquired from 1 Hz to 1 MHz with a resolution bandwidth of 5 % and a cross-correlation factor of 100. Fig. 3 contains the results of measurements of the RF generator at 20 GHz with and without referencing to the Rb reference clock. These measurements are within run-to-run deviation for offset frequencies above 15 Hz with a phase noise of -114.9 dBc/Hz at 1 MHz. For frequencies below 15 Hz the phase noise of the referenced RF generator is up to 13 dB better. The measurements of the EO comb at 40 GHz using the second mode show the same behaviour with and without reference and reach a phase noise of -108.7 dBc/Hz at 1 MHz. Fig. 3 additionally contains the amplitude noise of the EO comb at 40 GHz using the second mode. The amplitude noise is at least 10 dB and typically 25 dB smaller than the phase noise throughout the spectrum. Amplitude noise will therefore be neglected in the following. We conclude that referencing to the Rb clock only impacts the phase noise below $\sim$ 100 Hz. We still employ it for all of the following measurements.

4.3. Side mode scaling of the phase noise

We compare the scaling of the phase noise at an RF of 10 GHz between the modes one to four. Fig. 4 a) shows the difference between the phase noises from modes two to four compared to mode one. The noise contributions show substantial differences depending on the offset frequency. In the high frequency end, above 13 kHz, the noise scales almost exactly quadratically. For convenience we added horizontal lines corresponding to exact quadratic scaling. Fig. 4 b) depicts the average

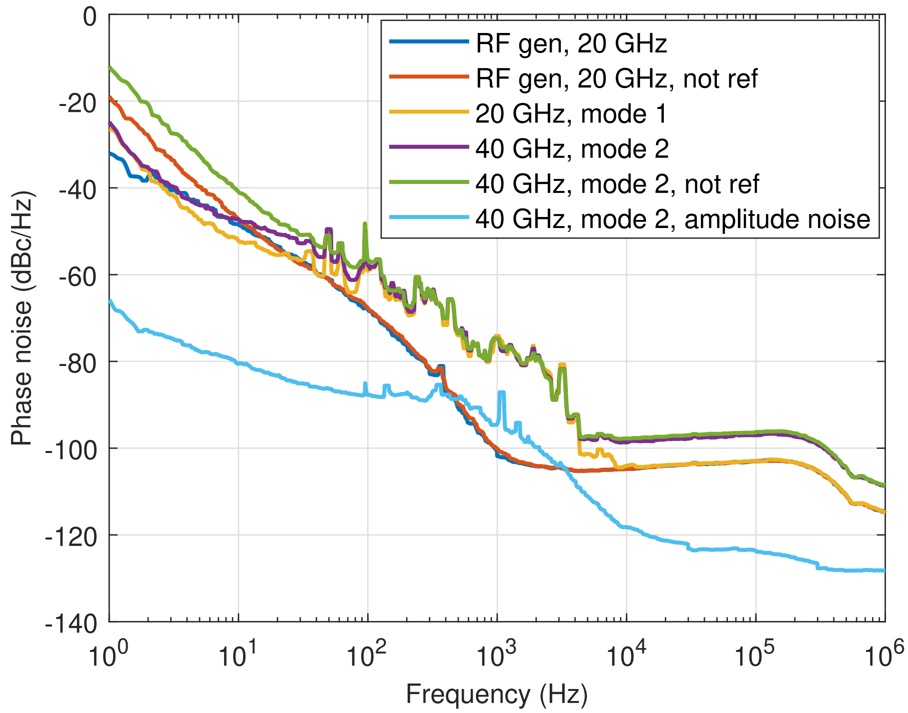

Fig. 3. Measured phase noise of the RF generator at 20 GHz and the EO comb at 40 GHz, both with and without referencing to the Rb clock. Additionally, the EO comb at 20 GHz and the amplitude noise at 40 GHz is shown.

noise between 15 kHz and 1 MHz with a maximum deviation of 0.5 dB from quadratic scaling. $L_{\mathrm{RF}}(f)$ dominates the phase noise in this part of the noise spectrum. For offset frequencies between 100 Hz and 4 kHz external noise sources dominate the spectral noise and possibly some minor contributions from $L_{\mathrm{opt}}(f)$ as the phase noise shows hardly any dependency on the mode order. Some of this phase noise is generated by the fans of the devices, other acoustic sources and potentially vibration. The phase noise differences between 5 Hz and 100 Hz show mode dependent but sub-quadratic behaviour. This is caused when the phase noise of both $L_{\mathrm{RF}}(f)$ and $L_{\mathrm{opt}}(f)$ are similar in size. Together with the findings from Fig. 3 we conclude that the dominant noise source is the phase noise of the RF generator, except between 100 Hz and 4 kHz. If even higher optical modes than shown here are used, $|m|^2 L_{\mathrm{RF}}(f)$ will eventually become the main contributor to the phase noise and we expect purely quadratic scaling.

4.4. Combined scaling

A difference frequency of 40 GHz can be achieved by a multitude of RF and mode combinations (Tab. 1). Fig. 5 shows the resulting phase noises for the modes two to four. The phase noises have a typical difference of less than 1 dB. Larger differences of up to 4 dB occur at 575 Hz, close to 1 Hz, and above 500 kHz. All three phase noises are basically the same. In the end, only the total multiplication factor matters, irrespective of whether multiplication ocurred in the RF domain or as higher EO side band order.

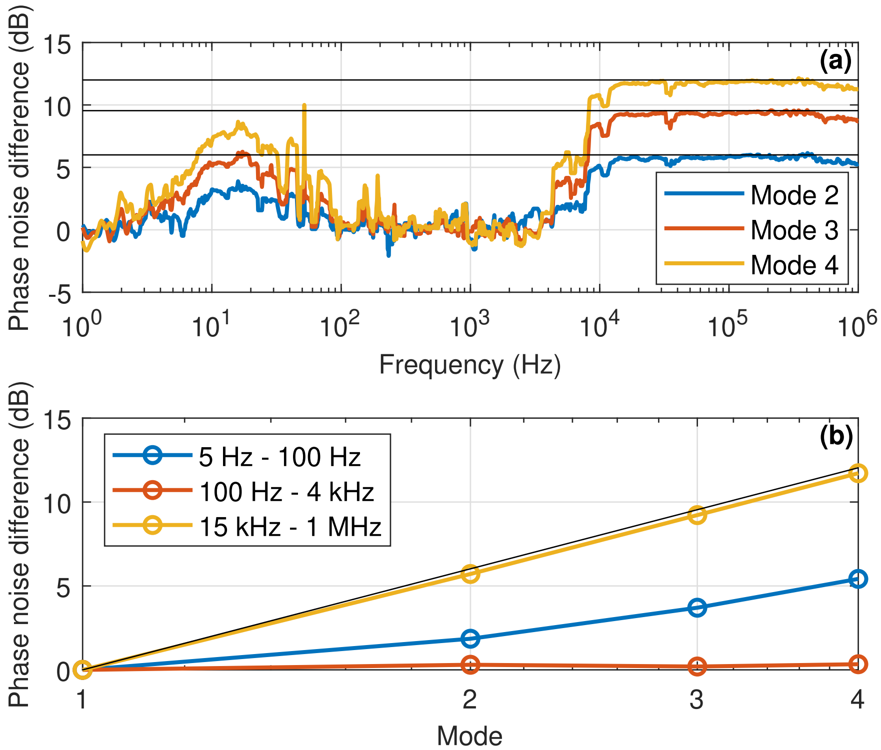

Fig. 4. a) Differences of the measured phase noise of the modes 2 to 4 compared to the mode 1 using a RF of 10 GHz with solid black lines for the corresponding fully quadratic scalings, b) scaling of the noise with mode number for different spectral ranges with a black line representing fully qudratic scaling.

5. Conclusion

We investigated the phase noise of an electro-optical comb for photonic millimeter wave and terahertz generation. We have proven a competitive phase noise of -108.7 dBc/Hz at an offset frequency of 1 MHz at a center frequency of 40 GHz. For low offset frequencies, the phase noise scales sub-quadratically with the electro-optical mode but approaches a quadratic scaling for offset frequencies above $\sim$ 15 kHz. The phase noise of the generated millimeter-wave or THz frequency is mainly determined by the phase noise of the driving RF generator plus 6dB for each time the RF is electro-optically multiplied by a factor of 2. In that context, it does not make a difference whether this multiplication is happening in the optical domain by using higher order modes or in the RF domain. Except for a small window between 100 Hz and a few kHz where the phase noise was dominated by external sources the noise of the spectral purity and stability of the radio frequency generator limits the phase noise performance. An RF generator with a lower phase noise would immediately reduce the millimeter wave and Terahertz phase noise. We remark that locking to a Rubidium clock only affected offset frequency components below $\sim$ 100 Hz. The proposed EO comb system is well suited as an extension module for electronic measurement equipment. We remark that higher frequencies deep into the THz range had already been demonstrated with EO combs in the literature. The maximum frequency of 40 GHz investigated in this manuscript was solely dictated by the frequency coverage of the phase noise analyzer.

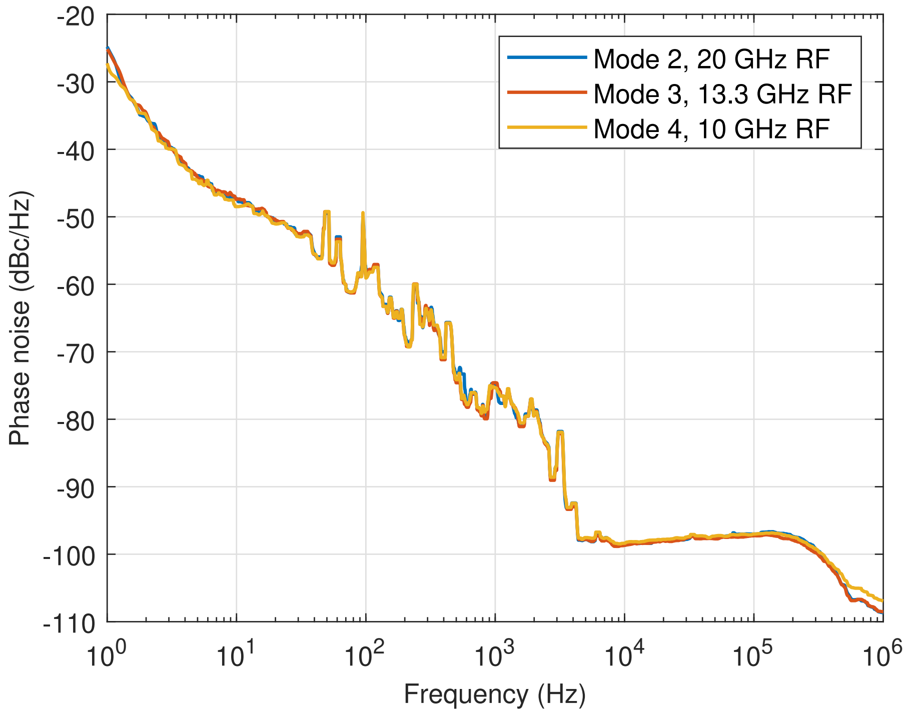

Fig. 5. Measured phase noise of the EO comb at 40 GHz, generated with different EO modes.

Funding. This work was supported by the European Research Council (ERC) Proof-of-Concept "PhoSTer-THz" under Grant 101057162, the collaborative research center SFB-TRR 196 "MARIE" funded by the German research foundation (project number 287022738) and by the federal ministry of education and research, Germany (BMBF) through "6GEM" (grant 16KISK039).

Acknowledgments. We thank Jan Balzer and his group from the University of Duisburg-Essen for lending us two of their variable optical delay lines for the duration of the measurements.

Disclosures. The authors declare no conflicts of interest.

Data Availability Statement. Data underlying the results presented in this paper are available in Ref. [27].

References

1. W. Harris, "The application of superheterodyne frequency converison systems to multirange receivers," Proc. Inst. Rádió Eng. **23**, 279–294 (1935).
2. C. Risacher, R. Güsten, J. Stutzki, *et al.*, "The upGREAT dual freuqency heterodyne arrays for SOFIA," J. Astron. Instrum. **7** (2018).
3. R. A. Witte, *Spectrum and Network Measurements* (SciTech Publishing, 2014), 2nd ed.
4. H.-W. Hübers, "Terahertz heterodyne receivers," IEEE J. selected topics quantum electronics **14**, 378–391 (2008).
5. M. Tiebout, *Low Power VCO Design in CMOS* (Springer, 2005).
6. A. A. Sweet and R. Parrott, "A wide band, low phase noise, differential YIG tuned oscillator," in *WAMICON,* (IEEE, Tampa, FL, USA, 2014).
7. W. Kruiskamp, "A fully differential 40 MHz switched-capacitor crystal oscillator with fast start-up," in *ESSCIRC,* (IEEE, Milan, Italy, 2022).
8. K. Suzuki, Y. Abe, N. Ishihara, *et al.*, "Small-sized rubidium oscillator," in *IEEE International Frequency Control Symposium,* (IEEE, Pasadena, CA, USA, 1998).
9. Z. Li and S. Zhang, "A 32 GHz two-stage frequency synthesizer with 100 MHz reference using injection locked technology," in *ECNCT,* (IEEE, Guangzhou, China, 2023).

10. U. Soylu, A. Alizadeh, M. Seo, and M. J. W. Rodwell, “280-GHz frequency muliplier chains in 250 nm InP HBT technology,” IEEE J. Solid-State Circuits **58**, 2421–2429 (2023).
11. P. Heymann and M. Rudolph, *A Guide to Noise in Microwave Circuits* (John Wiley & Sons, Inc, Hoboken, NJ, USA, 2022).
12. M. Kadam, F. Padovan, and V. Issakov, “Dual-core mm-wave VCO with enhanced second harmonic extraction by mode separation,” in *IEEE 23rd Topical Meeting on Silicon Monolithic Integrated Circuits in RF Systems,* (IEEE, Las Vegas, NV, USA, 2023).
13. Z. Zong, P. Chen, and R. B. Staszweski, “A low-noise fractional-N digital frequency synthesizer with implicit frequency tripling for mm-wave applications,” IEEE J. Solid-State Circuits **54**, 755–767 (2019).
14. H. Bello, L. Pantoli, H. J. Ng, *et al.*, “Low phase-noise high output power 176 GHz voltage controlled oscillator in a 130 nm BiCMOS technology,” IET Microwaves, Antennas & Propag. **13** (2019).
15. B. L. Krause, A. de Jesus Fernandez Olvera, and S. Preu, “Photonic spectrum analyzer for wireless signals in the THz range,” IEEE Access **10**, 42061–42068 (2022).
16. G. Gäumann and J. Morel, “Generation and measurement of traceable THz frequencies,” in *IRMMW-THz,* (IEEE, Paris, France, 2019).
17. A. Theis, M. Kocybik, G. von Freymann, and F. Friederich, “Free-space terahertz spectrum analysis with an optoelectronic hybrid system,” IEEE Trans. on Terahertz Sci. Technol. **13** (2023).
18. N. Kuse, K. Nishimoto, Y. Tokizane, *et al.*, “Low phase nosie THz generation from a fiber-referenced kerr microresonator soliton comb,” arxiv.org (2022).
19. T. Eichler, T. Puppe, S. Müller, *et al.*, “Ultra-stable tunable THz system for 6G communication based on photonics,” in *European Microwave Conference,* (Berlin, Germany, 2023).
20. A. de Jesus Fernandez Olvera, B. L. Krause, A. Betancur-Pérez, *et al.*, “Frequency selective optoelectronic downconversion of a terahertz pulse using ErAs:In(Al)GaAs photoconductors,” IEEE Access **9**, 95391–95400 (2021).
21. A. de Jesus Fernandez Olvera, B. L. Krause, and S. Preu, “A true optoelectronic spectrum analyzer for millimeter waves with Hz resolution,” IEEE Access **9**, 114339–114347 (2021).
22. T. A. Puppe, Y. Mayzlin, J. Robinson-Tait, and R. Wilk, “Comb-locked frequency-domain terahertz spectrometer,” in *IRMMW-THz,* (IEEE, Paris, France, 2019).
23. E. Prior, C. de Dios, R. Criado, *et al.*, “1 THz span optical frequency comb using VCSELs and off the shelf expansion techniques,” in *CLEO,* (IEEE, San Jose, CA, USA, 2016).
24. H. J. Tiziani, “Heterodyne interferometry using two wavelengths for dimensional measurements,” in *Laser interferometry IV: computer aided interferometry,* (SPIE, San Diego, CA, USA, 1991), pp. 490–501.
25. G. B. Arfken, H. J. Weber, and F. E. Harris, *Mathematical methods for physicists* (Academic Press, Boston, MA, USA, 2013), seventh ed.
26. M. Vidmar, “Extending Leeson’s equation,” J. Microelectron. Electron. Components Mater. **51**, 135–146 (2021).
27. B. L. Krause, A. Lavrič, J. Tebart, *et al.*, “Measurement data - phase noise of an electro-optical phase modulator based electro-optical comb,” (2024).

Appendix A: Correlated phase noise

SSB phase noise $L(f)$ is proportional to the square phase fluctuation $\phi(f)$. Translating it to the time domain leads to

$$\mathcal{F}^{-1}((\phi(f))^2) = \phi(t) * \phi(t) = \int_{-\infty}^{\infty} \phi(t')\phi(t-t')dt'$$

In case of correlated noise $\phi(t) = \phi_\mathrm{c}(t) - \phi_\mathrm{c}(t-\tau)$ leading to

$$\begin{aligned}
\mathcal{F}^{-1}((\phi_\mathrm{c}(f))^2) &= [\phi_\mathrm{c}(t) - \phi_\mathrm{c}(t-\tau)] * [\phi_\mathrm{c}(t) - \phi_\mathrm{c}(t-\tau)] \\
&= \int_{-\infty}^{\infty} [\phi_\mathrm{c}(t') - \phi_\mathrm{c}(t'-\tau)][\phi_\mathrm{c}(t-t') - \phi_\mathrm{c}(t-t'-\tau)]dt' \\
&= \int_{-\infty}^{\infty} \phi_\mathrm{c}(t') - \phi_\mathrm{c}(t-t')dt' - \int_{-\infty}^{\infty} \phi_\mathrm{c}(t') - \phi_\mathrm{c}(t-t'-\tau)dt' \\
&- \int_{-\infty}^{\infty} \phi_\mathrm{c}(t'-\tau) - \phi_\mathrm{c}(t-t')dt' + \int_{-\infty}^{\infty} \phi_\mathrm{c}(t'-\tau) - \phi_\mathrm{c}(t-t'-\tau)dt'
\end{aligned}$$

If $\tau = 0$, then

$$\mathcal{F}^{-}1((\phi_{\mathrm{c}}(f))^2)|_{\tau=0} = \int_{-\infty}^{\infty} \phi_{\mathrm{c}}(t') - \phi_{\mathrm{c}}(t-t')dt' - \int_{-\infty}^{\infty} \phi_{\mathrm{c}}(t') - \phi_{\mathrm{c}}(t-t')dt'$$
$$- \int_{-\infty}^{\infty} \phi_{\mathrm{c}}(t') - \phi_{\mathrm{c}}(t-t')dt' + \int_{-\infty}^{\infty} \phi_{\mathrm{c}}(t') - \phi_{\mathrm{c}}(t-t')dt' = 0$$

and if τ is significantly larger than the coherence time of the laser, then the two components of the correlated noise can be seen as independent components and sum to $2(\phi(f))^2$.